
New Folder Name

Construction and Commissioning

Construction and commissioning of the alternating-gradient synchrotron booster ultrahigh vacuum system

H. C. Hseuh, M. Mapes, B. Shen,^{a)} and R. Sikora
Brookhaven National Laboratory, Upton, New York 11973

(Received 30 September 1991; accepted 18 November 1991)

The recently completed alternating-gradient synchrotron booster is a synchrotron for the acceleration of both protons and heavy ions. To minimize the beam loss due to charge exchange of the partially stripped, low β ($=v/c$), very heavy ions with the residual gas molecules, ultrahigh vacuum of 10^{-11} Torr is required for the 200 m booster ring. An average pressure of mid 10^{-11} Torr has been achieved and maintained after initial *in situ* bakes and commissioning. In this article we describe: (1) design and layout of the vacuum systems; (2) material selection and vacuum processing; (3) personal computers/programmable logic controllers based bakeout system; (4) operation of vacuum instrumentation over long cable length; (5) results of bakeout and evaluation; and (6) experience gained during construction and commissioning.

I. INTRODUCTION

The recently completed alternating-gradient synchrotron (AGS) booster at Brookhaven is a small synchrotron of 200 m in circumference located between the existing 200 MeV Linac, the Tandem Van de Graaff and the alternating-gradient synchrotron (AGS). The construction was completed in early June, 1991 with the beam commissioning immediately following. The major objectives of the Booster are:

- (1) to increase the proton intensity in the AGS by a factor of 4, to 6×10^{13} particles per pulse (ppp),
- (2) to increase the AGS polarized proton intensity by a factor of 20 to 10^{12} ppp,
- (3) to accelerate partially stripped heavy ions up to gold (Au) in the Booster for the AGS and eventually for the relativistic heavy ion collider currently under construction at Brookhaven.

It is the third objective which puts the most stringent requirements on the vacuum system of the booster ring. In heavy ion accelerators, the cross sections for charge exchange (electron stripping and electron capture) between partially stripped, low β , very heavy ions and the residual gas molecules are usually rather large. They were calculated, as detailed in Ref. 1, by using empirical formulae which give the best fit to the measured cross sections. At the design vacuum of 3×10^{-11} Torr (90% H₂ and 10% CO), the integrated beam loss during acceleration cycles is less than one percent for Au⁺³³ at $E_{inj.} = 1$ MeV/amu, which has the largest cross sections of all the ion species to be accelerated in the booster. At a vacuum of 3×10^{-10} Torr (10% H₂ and 90% N₂), the beam loss for Au⁺³³ is calculated to be over 30%.

II. VACUUM SYSTEMS

The booster ring, with a circumference of 201.8 m, has 36 half-cells and 12 quarter-cells. The half-cells consist of dipole, quadrupole, and sextupole magnets. The 12 "missing dipoles" downstream of quarter-cells house the radio-frequency accelerating cavities, kickers and other beam components. The ring, as shown schematically in Fig. 1, is

grouped into seven vacuum sectors with each sector isolatable with all-metal gate valves. There are three beam transport lines, with a total length over 500 m, for injection of protons and heavy ions, and for extraction to AGS. The transport lines are designed for 10^{-10} – 10^{-9} Torr, which serve as a pressure differential between the 10^{-11} Torr ring and the existing 10^{-8} – 10^{-7} Torr vacuum of Linac and AGS. The design of the booster vacuum system can be found in Ref. 2. Some major components are described below.

A. Vacuum chamber

A typical half-cell chamber is shown in Fig. 2. It is 4.2 m long, made mostly of Inconel 625 and consists of chambers for dipole, quadrupole, pickup electrodes (PUEs), sextupole, bellows and a transition with ports connecting to pumps, gauges, and roughing valve. The dipole chambers are 2.8 m long with an elliptical cross section of 165×70 mm and are curved to a radius of 13.75 m and are 2.8 m in length. To compensate for the chamber eddy current effect during magnet ramping, six pairs of correction coils are mounted on the top and bottom of dipole chamber.

Conflat type flanges with 90° knife edges³ made of 316LN stainless steel are used throughout the ring vacuum system. To prevent recrystallization⁴ of pure copper gaskets after repeated high temperature bakes, all gaskets were made of copper alloyed with 0.1% Ag. Quick disconnect type flanges such as the EVAC⁵ and the inhouse developed 13 in. "chain-clamp" flanges, both featuring 90° Conflat knife edges are used at areas with high expected residual radiation. They were repeatedly baked to 300 °C with no creeping or leakage.

The PUE location has to be accurate within 0.1 mm after vacuum firing and repeated *in situ* bake. This leads to the double gimbaled suspension² which allows the electrodes to be rigidly supported while being free to move radially and longitudinally during vacuum firing or bakeout. The position accuracies achieved were within ± 0.1 mm in the transverse directions and less than 1 mrad in rotation.

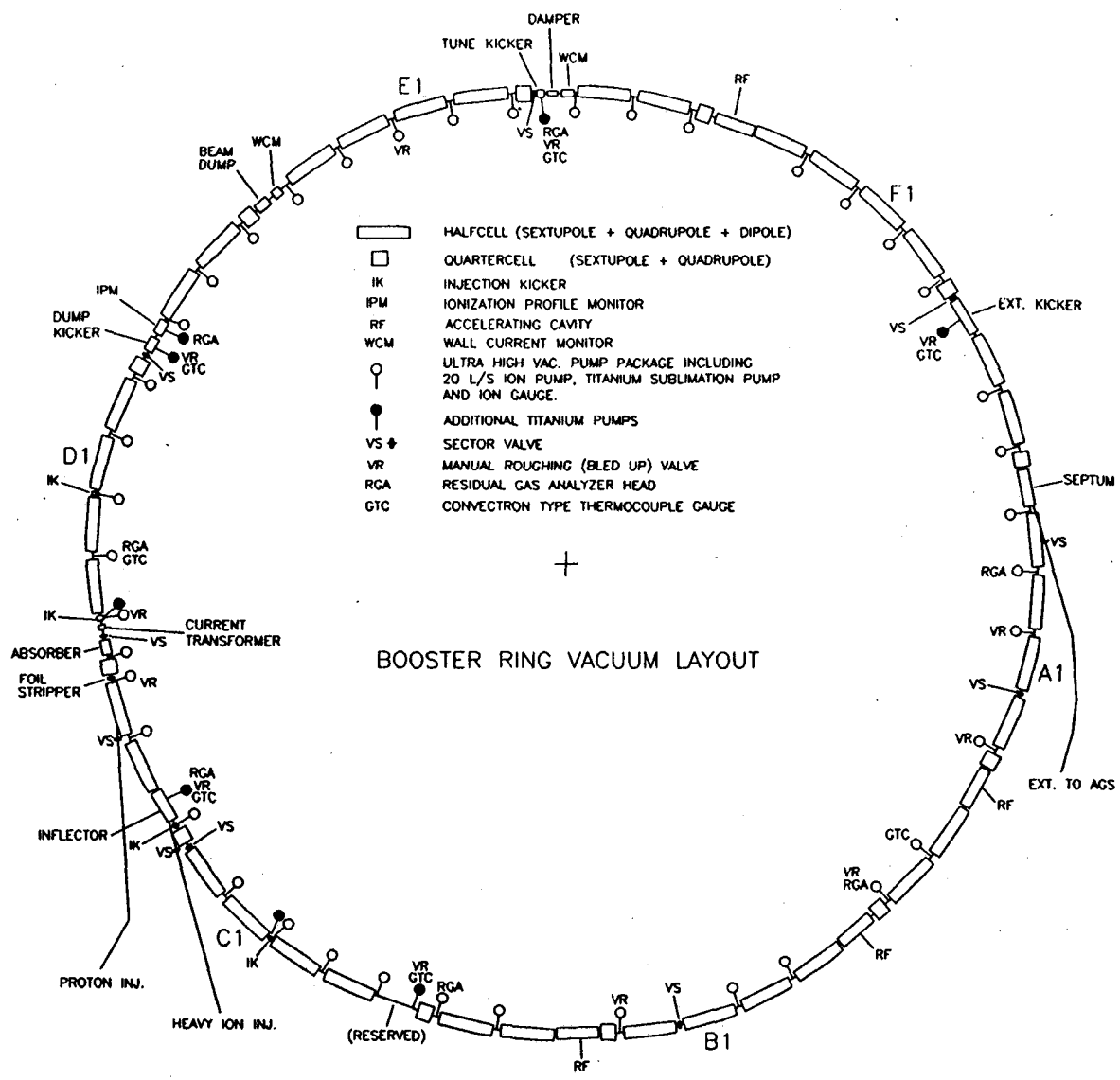


FIG. 1. Booster ring vacuum layout.

B. Vacuum pump

The ring vacuum was achieved by the combination of titanium sublimation pumps and ion pumps. Fifty five titanium cartridges with three filaments each are mounted in the pump bodies. The pump body with a 3000 cm² area for sublimed titanium has approximately 1000 ℓ /s pumping speed for active gases. The nongetterable gases such as methane and argon are removed by small ion pumps. Ion pumps and nonevaporable getter pumps⁶ are used in the beam transport lines. Portable turbopump stations were used during roughing down, bakeout, and conditioning of the vacuum sectors.

C. Bakeout

The vacuum chambers and the components within were designed to be *in situ* bakeable to 300 °C. Thermocouples (TCs) and custom heating blankets were installed on the chambers before assembling into magnets. Kapton

wrapped *E*-type TCs were used for its low magnetic permeability. The blankets have parallel redundant heating elements, made of multiple strand nickel-copper alloy wires, and fiberglass insulating jackets. The tight space between magnet pole tips and chambers limits the thickness of most blankets to no more than 6 mm. The large heat loss to the magnets due to this thin insulation necessitated the circulating of magnet cooling water during the bake. Heating blankets not confined by space requirement vary from 10 to 25 mm in thickness.

The bakeout of each vacuum sector was controlled and monitored with portable personal computer (PC)-based programmable logic controllers (PLC). The blankets and TCs of each half-cell were terminated to local contactor boxes, which were then connected to PLCs prior to bake. Each PLC cart has modules to monitor up to 150 TCs and control up to 100 corresponding processes, such as heating blankets. The PC downloads and initiates the programmed

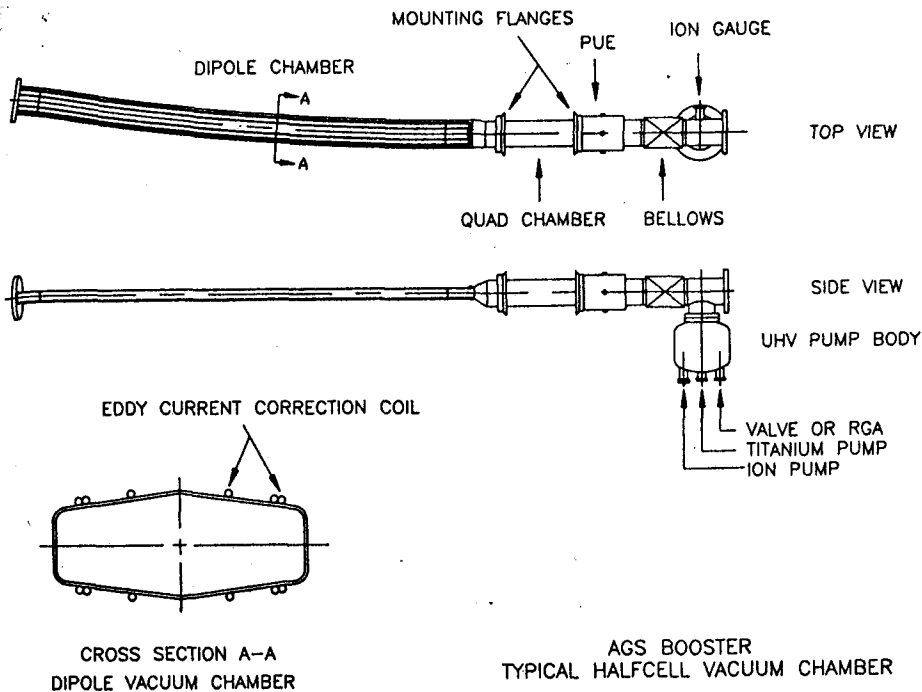


FIG. 2. Schematics of half-cell vacuum chamber; the heating blankets are not shown.

bake cycles and database to PLCs, and also alarms the operators when abnormal or failure conditions occur. With one PC and four PLCs, two thirds of the ring can be baked at one-time with each sector having its own programmed bake cycle.

D. Instrumentation

Various vacuum instrumentations are needed to power the pumps, monitor and protect this ultrahigh vacuum system. Due to the presence of high radiation levels in the booster tunnel, all power supplies and controls are located in a separate instrumentation building. This includes power supplies for ion and titanium pumps, controllers for vacuum gauges and valves, and the computer systems. The

layout of instrumentation is shown schematically in Fig. 3. The commercial gauge controllers communicate with the device controllers (D/Cs) through RS232 links. The ion pump power supplies and valve controllers are linked to the D/Cs through an IEEE-488 compatible interface. The D/Cs communicate with the Apollo nodes via station drops. The SCR (silicon controlled rectifier) based titanium pump power supplies are operated manually, since they are energized periodically for only a few minutes.

The titanium pump power supplies degas the titanium filaments during pump down and bakeout, and sublime titanium onto the pump body surfaces when the need arises. These supplies consist of SCR based controllers which power and regulate the sublimation rate using a constant current mode. The current of SCR controllers is stepped up by transformers located near the cartridges. By calibrating the gain and offset pots of each SCR controller versus the transformer ratios, current stability of better than $\pm 2\%$ is achieved during sublimation at 48 A. The sublimation rate is approximately 1 mg/min. One gram of titanium is available from each filament before it breaks.

The dual ion pump power supplies, using ferroresonant transformers, develop potentials up to 5 kV and current up to 200 mA. Both voltage and current are measured for pressure monitoring and for diagnostics. Current down to 10 μ A can be reliably measured through the linear and log amplifiers. Relay outputs are available to interlock the sector valves and other equipment.

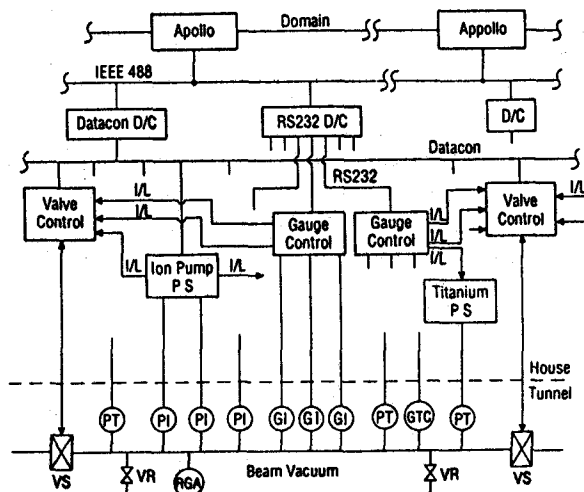


FIG. 3. Layout of the vacuum instrumentation and control.

E. Vacuum monitoring

The vacuum is monitored by Pirani gauges, ion gauges, ion pump currents, and residual gas analyzers (RGAs). The Pirani gauges cover from atmosphere to 1×10^{-4} Torr. The ion pump current can be used to measure pres-

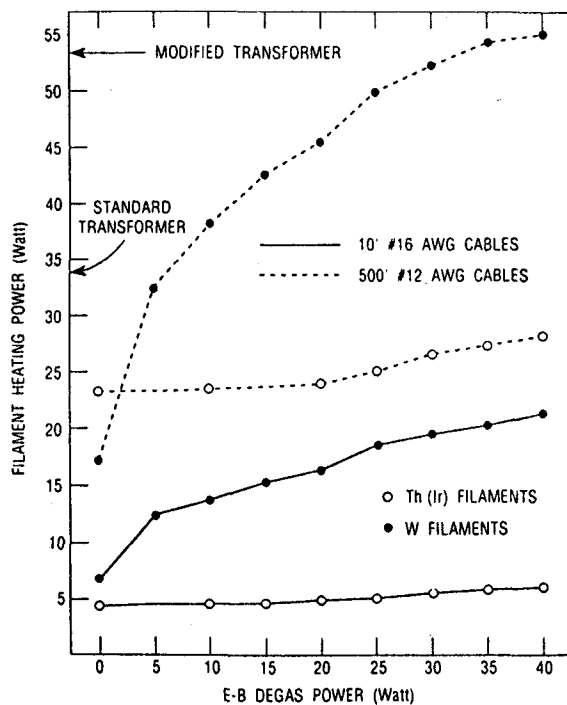


FIG. 4. Filament heating power vs degassing power over long cable length. The emission was 1 mA at zero degassing power.

sure down to 10^{-9} Torr. The nude Bayard-Alpert gauges (BAGs) measure vacuum from 10^{-3} Torr down to high 10^{-12} Torr. These BAGs have a thin collector of 0.05 mm diam. The sensitivities and equivalent x-ray limits of some of these BAGs were measured⁷ to be 20 ± 2 Torr⁻¹ and $(4 \pm 1) \times 10^{-12}$ Torr, respectively for nitrogen, by comparing with a calibrated⁸ extractor gauge and a modulated BAG. The inverted magnetron cold cathode gauges were tested and found to be unreliable at 10^{-11} Torr due to periodical extinguishment of discharge.

The BAGs were mounted near the ultrahigh vacuum (UHV) pump bodies in the standard half-cells and at the center of the beam component boxes. The pressure distribution along the half-cell chambers can be expressed by:

$$P(x) = P_0 + q(L/S + L^2/4c - x^2/c),$$

TABLE I. Noise pickup of long coaxial cables.

Cable type	Vacuum/environment ^a	Microphonics ^b	
RG 59 A/U, 1000 ft	5×10^{-11} in lab	+ 20%,	- 20%
RG 59 A/U, 650 ft	5×10^{-11} in AGS w/rf	+ 200%	- 100%
RG 59 A/U, 650 ft	5×10^{-11} in AGS w/o rf	+ 25%	- 25%
RG 59 A/U, 650 ft triaxial	3×10^{-11} in AGS w/rf	+ 30%,	- 30%
Beldon 9223, 500 ft	4×10^{-11} in AGS w/rf	+ 100%,	- 50%
Beldon 9311, 500 ft	5×10^{-11} in AGS w/rf	+ 30%,	- 20%
Beldon 9311, 500 ft	2×10^{-11} in AGS w/rf	+ 50%,	- 50%
Beldon 9311, 500 ft	2×10^{-11} in AGS w/o rf	+ 30%	- 30%

^aVacuum in Torr; AGS = cabling from power supply house to UHV chamber in AGS tunnel; rf = both magnets and cavities ramping.

^bThe percentages of microphonics are derived from the range of vacuum readings divided by the true vacuum readings taken locally with a 10 ft cable.

P_0 is the base pressure of the pump, c the linear conductance of the chamber, q linear outgassing, S the pumping speed, and L the distance between pumps. The linear conductance of a half-cell chamber is approximately 1×10^5 l/cm/s. With an estimated pumping speed of 1000 l/s at the neck of the pump and 4.2 m between pumps, the average pressure in the half-cell chambers, by integrating the above equation, is approximately 1.3 times of the BAG readings near the neck of the pump. This ratio is not very dependent on the outgassing rate of the chamber walls and the half-cell chamber pressure turns out to be insignificant in measuring the ring average pressure. The vacuum readings at some beam components, as measured directly by the BAGs, were one or two decades higher than those of half-cell chambers and became the dominant part of the average pressure.

One quadrupole type RGA head was installed in each ring sector. Each head is powered with a portable controller when there is access to the tunnel. With electron multipliers, the RGAs have partial pressure sensitivities down to 10^{-14} Torr level. They were installed as received from manufacture without further calibration and are used to identify qualitatively the composition of residual gas species in the ring vacuum sectors.

Commercial vacuum process controllers (VPCs) are used to power the gauges. The VPCs have process control channels which are assigned either to ion gauges or Pirani gauges. Through these channels, the Pirani gauges interlock the turning on of the ion gauges, ion pumps, and titanium pumps in the same sectors. The ion gauges provide interlocks for sector valves and beam components.

The output voltage from the standard transformers of the VPCs is not sufficient to power the ion gauge filaments over long cable lengths (up to 650 ft). This is overcome by using American Wire Gauge (AWG) no. 12 wires and transformers with a 40% higher output voltage in the VPC. Figure 4 gives the measured filament heating power during electron bombardment (EB) degassing for two cable lengths and for two types of gauge filaments. The standard transformers with 13 V ac output can only degas thoriated iridium filaments over a long cable length. The modified transformers have 19 V output and allow the degassing of a tungsten filament with up to 35 W over 500 ft of no. 12 AWG cables.

TABLE II. Cleaning and vacuum firing of beam components.

Material	Chemical cleaning	Vacuum firing	
		Temp (°C)	Duration (h)
Stainless/Inconel	Detergent	950	2
		Or 500	24
Welded bellows	Alcohol soak	500	24
Ferrite	Alcohol soak	400	50
Feedthroughs	Alcohol soak	500	2
Ceramic w/brazing	Alcohol soak	500	2
Graphite	Alcohol soak	950	2
Copper	Phosphate dip	500	24

At low 10^{-11} Torr vacuum, the gauge collector current is only a few picoamperes, which is susceptible to noise pickup especially over long cable lengths and results in erratic pressure readings. Two prominent sources of noise in accelerator environment are the electromagnetic interference (EMI) from magnets and power supplies; and the radio-frequency interference (RFI) from accelerating cavities. Tests of noise pickup over long cable runs in the AGS ring, during machine operation, were carried out. The results are summarized in Table I. Regular RG-59 coax has effective shielding around 90% as compared with that of Beldon 9311 cables. At mid 10^{-11} Torr, the microphonics of RG-59 is usually 100% of the vacuum readings taken with ten feet of cable. To minimize EMI/RFI, Beldon 9311 cables are used. This cable has microphonics of approximately 30% of the vacuum readings at mid 10^{-11} Torr and is acceptable for booster vacuum operation. This coax features 100% shield coverage, a foil/braid outer shield, a polyethylene dielectric of 26 pf/ft, and good dc performance. The grid and filament wires (four each, 12 AWG) are also placed in a single twisted, shielded, low smoke, and radiation retardant jacket.

F. Valve control and interlock

The beam vacuum is protected by sector valves, which are interlocked by gauges and ion pumps through process control channels and TTL, respectively. A fault detected by any two out of four ion gauges and ion pumps in the same sector will cause the valves at both ends of the sector to close, thus minimizing the loss of vacuum in adjacent sectors. This voting scheme minimizes false triggering due to noise or malfunctioning of individual devices. A fast closing valve with a closing time of less than 15 ms is installed between the Linac and the booster to protect the booster ultrahigh vacuum ring from potential catastrophic failure at Linac. To prevent beam from damaging valves, the valve-closing signals trigger the fast beam interrupt system located at the ion source within 350 μ s. Auxiliary interlock input/output (I/Os) in the valve controllers also allow for interlocking other valves or equipment.

III. CONSTRUCTION AND COMMISSIONING

A. Vacuum processing

To reduce outgassing, various degassing treatments were applied to vacuum chambers and beam components. Before assembly, all chambers and parts were chemically cleaned. The chemical cleaning consisted of vapor degreasing, water rinse, alkaline detergent soak, and water rinses. The parts were welded and assembled in a Class 1000 clean room before vacuum firing. The chambers were usually vacuum fired at 950 °C for 2 h at vacuum of low 10^{-5} Torr.

The treatment of beam components, depending on the material involved and the assembly/testing sequence, could be quite different. To prevent entrapment of cleaning fluid, ferrites, graphites, and other ceramic components are cleaned by vapor degreasing and soaking in an ultrasonic alcohol bath. The nickel-zinc ferrites used in the kicker magnets have outgassing rates of 1×10^{-12} Torr $\ell/s \text{ cm}^2$ after vacuum firing at 950 °C. However, due to the decomposition of oxides at high temperature which reduced the ferrite impedance, the ferrite was fired at 400 °C. The dimensions of some beam components exceeded the capacity of the inhouse vacuum furnace, therefore, had to be fired separately before assembly. Pressurized steam was also used to clean a few assembled beam components, which were contaminated during assembly. The firing temperatures and cleaning steps for some components are listed in Table II.

B. Vacuum evaluation

The assembly and vacuum evaluation of half-cells began in March, 1990, when the first set of production magnets was available. The tunnel was ready for component installation in June, 1990. The assembly and testing of beam components began during the summer of 1990. All ring components were installed by April, 1991. The pump down and bakeout of the sectors began in Jan., 1991, when all the components in the first sector were installed. The vacuum system was completed in June, 1991.

All the vacuum chambers and the beam components were designed to be bakeable to 300 °C. They were baked at 250 °C before installation and at 200 °C *in situ*, which was adequate to achieve the designed base vacuum.

After cleaning, welding, and vacuum firing, eddy current coils, thermocouples and heating blankets were mounted on the half-cell chambers. The chambers were then inserted into the prealigned magnets and the PUEs were aligned against the quadrupoles. Of the thirty-six half-cell chambers, two had to be reworked to meet the ± 1 mrad rotational tolerance of the PUEs. The downstream vacuum flange was welded after PUE alignment and electrical test. The associated vacuum components, pumps, gauges, valve, and residual gas analyzer, were then mounted for pump down and bakeout. The bakeout began on day 1 and terminated on day 3. Degassing, conditioning, and energizing on of the pumps followed. Before qualifying for installation, the half-cells, with their associated UHV pumps, had to reach vacuum of $< 1 \times 10^{-10}$ Torr



FIG. 5. Completed half-cell before installation.

and be hydrocarbon free. Approximately eighty percent of the chambers reached a vacuum better than 5×10^{-11} Torr one day after bake. Half of the chambers with higher pressure were found to have leaks at the Conflat flange joints. Two chambers had leaks at the welds and were repaired. A half-cell ready for installation is shown in Fig. 5.

Every beam component for the ring was evaluated for UHV before installation. Among the twenty beam components tested, ten had reached vacuum of 10^{-11} Torr one day after bake. Two kickers had to be rebaked at higher temperature (300°C) for several days to remove hydrocarbon contamination introduced during the assembly. Others had high hydrogen outgassing originating from parts that were not vacuum fired.

The *in situ* bakes of vacuum sectors, similar to half-cell bakeouts, also spanned three days. The beam transport line sectors were baked from 100 to 150°C , while the ring sectors were baked at 200°C . A vacuum from 10^{-10} to 10^{-9} Torr was reached in the lines, depending on bake temperature and available pumping speed. Among the seven ring sectors, three reached the designed vacuum of low 10^{-11} Torr one day after bake. One sector had hydrocarbon contamination and had to be rebaked at 250°C for five days. After initial bakes, the ion gauge readings in two thirds of the ring were at 1×10^{-11} Torr (the readout limit of our VPCs) and an average vacuum of high 10^{-11} Torr was reached. Using RGAs, sources of local pressure bumps were identified as either high hydrogen

outgassing at ferrite kickers or small leaks. We expect to reach the designed vacuum of 3×10^{-11} Torr when the kicker magnets are rebaked and the leaks are repaired. The RGAs allowed us to identify the leaks even at low 10^{-11} Torr level. This is evident as shown in Fig. 6, where the presence of argon peak ($m/e = 40$) in sector C indicates a leak which was subsequently located at a bellows weld.

IV. CONCLUSIONS

With proper selection of material (metal and ceramic), degassing treatment and *in situ* bake, a vacuum of 10^{-11} Torr was achieved over the 200 m booster ring. The selection of inconel 625 and stainless steel 316LN as chamber and flange material allow us to avoid chromium carbide precipitation during welding and vacuum firing. Carbide precipitation is susceptible to corrosion^{4,9} especially under radiation environment. No knife-edge rounding was observed after 950°C vacuum firing, attributed to the 90° knife-edge design.³ The commercial and the homemade quick disconnect flanges worked well after repeated thermal cyclings.

The use of PC/PLC based bakeout control system assists in monitoring and controlling the bakeouts of several sectors with minimum operator intervention. The SCR power supplies were found to be accurate within ± 1 A when subliming titanium through 500 ft of cable. The operation of ion gauges over long cable length was more complex than expected. The AWG #12 wires used to power

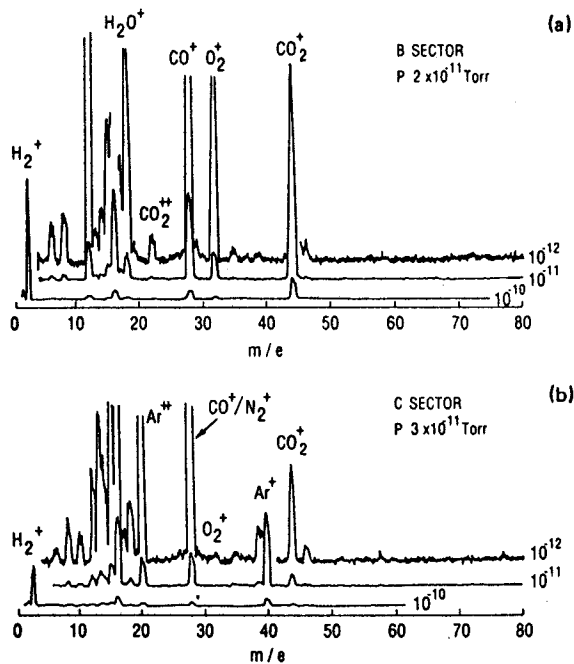


FIG. 6. Residual gas spectra of vacuum sectors at 10^{-11} Torr (a) without detectable leak; and (b) with 10^{-10} Torr ℓ/s leak at bellows. The leak is evident by the presence of argon at $m/e = 40$.

gauge filaments and modified transformers compensated for the voltage loss in the cables. The triac firing cycles of filaments had to be shielded from the collectors. The noise pickup of the collector cables was minimized by using fully

shielded low capacitance cable. However occasional oscillations in the gauge readouts during acceleration cycles limit their accuracy to around 50% at low 10^{-11} Torr. The use of RGAs as a diagnostic tool at ultrahigh vacuum levels proves to be very powerful in qualitatively identifying the sources of residual gas.

The tight space between the magnets and chambers, and the expected residual radiation will make the maintenance and upgrade of this vacuum system rather difficult. The bakeout system is necessary to reduce thermal outgassing and will also allow us to treat areas with contamination. The cost of the bakeout system, including blankets, TCs, contactor boxes, PLCs, PC and labor, is much higher than originally estimated and is approximately 30% of the total vacuum system cost. The procurement of custom blankets to fit chambers and beam components of various shapes and dimensions was especially costly and time consuming.

ACKNOWLEDGMENT

Work performed under the auspices of the U.S. Department of Energy.

¹Present address: Institute of High Energy Physics, Beijing, China.

²H. C. Hseuh *et al.*, IEEE 2669-0, 574 (1989).

³H. C. Hseuh, Vacuum 41, 1903 (1990).

⁴D. Edwards, Jr., D. McCafferty, and L. Rios, J. Vac. Sci. Technol. 16, 2114 (1979).

⁵W. Unterlerchner, J. Vac. Sci. Technol. A 5, 2540 (1987).

⁶Trade name of EVAC AG, Buch3, Switzerland.

⁷H. C. Hseuh *et al.*, Am. Inst. Phys. Conf. Proc. 171, 108 (1988).

⁸H. C. Hseuh and C. Lanni, J. Vac. Sci. Technol. A 5, 3244 (1987).

⁹This extractor gauge was calibrated through Leybold-Heraeus by Physikalisch-Technische Bundesanstalt, Berlin.

¹⁰J. P. Bacher and N. Hilleret, Vacuum 41, 1914 (1990).